Conference paper
UDC 538.911
DOI: https://doi.org/10.18721/JPM.171.120

Individual GaP nanowire conductivity studied with atomic force microscopy and numerical modeling

V.A. Sharov [1, 2] ✉, P.A. Alekseev [2], V.V. Fedorov [1], I.S. Mukhin [1]

[1] Alferov University, St. Petersburg, Russia;

[2] Ioffe Institute, St. Petersburg, Russia

✉ vl_sharov@mail.ru

Abstract. Growth strategies for achieving highly-doped GaP nanowires are investigated. Eight nanowire arrays are synthesized under different growth parameters via molecular beam epitaxy with the use of silicon and beryllium as *n*- and *p*- dopants. Electrical conductivity of individual nanowires from each array is investigated via conductive atomic force microscopy. The obtained current-voltage characteristics are numerically analyzed, the impact of nanowire geometry, contact properties and doping on the conductivity is estimated.

Keywords: nanowires, GaP, gallium phosphide, conductivity, doping, atomic force microscopy

Funding: This study was funded by Russian Science Foundation, grant 23-72-01082.

Citation: Sharov V.A., Alekseev P.A., Fedorov V.V., Mukhin I.S., Individual GaP nanowire conductivity studied with atomic force microscopy and numerical modeling, St. Petersburg State Polytechnical University Journal. Physics and Mathematics. 17 (1.1) (2024) 125–130. DOI: https://doi.org/10.18721/JPM.171.120

Материалы конференции
УДК 538.911
DOI: https://doi.org/10.18721/JPM.171.120

Исследование проводимости одиночных нитевидных нанокристаллов GaP с помощью атомно-силовой микроскопии и численного моделирования

В.А. Шаров [1, 2] ✉, П.А. Алексеев [2], В.В. Федоров [1], И.С. Мухин [1]

[1] Академический университет им. Ж.И. Алфёрова РАН, Санкт-Петербург, Россия;

[2] Физико-технический институт им. А.Ф. Иоффе РАН, Санкт-Петербург, Россия

✉ vl_sharov@mail.ru

Аннотация. С помощью проводящей атомно-силовой микроскопии получены вольтамперные характеристики одиночных нитевидных нанокристаллов фосфида галлия, легированных кремнием и бериллием, выращенных методом молекулярно-пучковой эпитаксии при различных условиях. Построена численная модель для расчета вольтамперных характеристик, оценено влияние на проводимость ННК их геометрии и легирования, а также подвижности носителей заряда и величины барьера Шоттки с зондом. На основании проведенного анализа установлены режимы роста, оптимальные для синтеза высоколегированных *n*- и *p*- ННК фосфида галлия.

Ключевые слова: нитевидные нанокристаллы, GaP, фосфид галлия, проводимость, легирование, атомно-силовая микроскопия

Финансирование: Работа выполнена при поддержке Российского Научного Фонда, проект № 23-72-01082.

Ссылка при цитировании: Шаров В.А., Алексеев П.А., Федоров В.В., Мухин И.С. Исследование проводимости одиночных нитевидных нанокристаллов GaP с помощью атомно-силовой микроскопии и численного моделирования // Научно-технические ведомости СПбГПУ. Физико-математические науки. 2024. Т. 17. № 1.1. С. 125–130. DOI: https://doi.org/10.18721/ JPM.171.120

Introduction

III-V semiconductor nanowires are promising as components of optoelectronic devices. In particular, gallium phosphide nanowires are prospective as nanophotonic waveguides and components of flexible light emitting diodes [1]. Despite the extensive worldwide research in the past decades, the commercial implementation of nanowires is still difficult. Today, doping control at the nanoscale is considered to be the last fundamental difficulty towards nanowire-based devices [2, 3]. In this work we investigate the doping control in GaP nanowires grown via molecular beam epitaxy (MBE) and study Be and Si behavior as dopants. We synthesize Be- and Si-doped GaP nanowire arrays and investigate the electrical properties of individual nanowires via complementary experimental and numerical techniques. First, the current-voltage characteristics (I–V curves) of vertical nanowires are obtained. Then, the doping level is estimated via numerical modeling of these curves. Importantly, herein we analyze individual nanowires rather than the averaged response from the whole arrays, providing more insights about nanoscale phenomena, which in fact determine the performance of macroscale nanowire array device.

Materials and Methods

Nanowire growth was carried out using Veeco Gen III MBE setup equipped with Si, Be and Ga effusion cells and valved phosphorous cracker cell. The nanowire arrays were synthesized on highly-doped (111) Si substrates via self-catalyzed vapor-liquid-solid (VLS) growth mechanism assisted by Ga droplet avoiding the use of foreign metal contamination, and thus providing lower impurity level and electrically active defects. Formation of GaP nanowires occurs at the pinhole defects of the silicon surface oxide facilitating the formation of catalytic Ga droplets required for vertical nanowire growth.

Conductive atomic force microscopy (C-AFM) was utilized to obtain I-V curves of individual nanowires using NT-MDT NTegra AFM setup and conductive probes with TiN and W2C coatings. The idea of the method is to use the grounded conductive probe as a top electric contact to an individual nanowire which is possible due to nanometer scale tip curvature radius and atomic scale positioning precision [4, 5]. The nanowire coordinates are preliminarily obtained in AFM scan. Bias voltage is then applied to the growth substrate, and the current passing through the nanowire is registered.

The numerical modeling was carried out in Silvaco Atlas finite element computational package, which is designed for semiconductor device simulations, solving Poisson's equation, carrier continuity equations and transport equations [6]. The proposed model possesses cylindrical symmetry, includes a nanowire with two electric contacts (bottom corresponds to GaP/Si heterobarrier, top to GaP/probe Schottky barrier). The simulation utilizes Klaassen model [7] describing band-to-band tunneling and Matsuzawa's Universal Schottky Tunneling model [8], describing the thermionic emission at the metal/semiconductor interface and the spatially distributed tunneling calculated at each semiconductor around the interface.

Results and Discussion

Eight samples were fabricated. SEM image of each sample as-grown are shown in Fig. 1. Samples 1–4 (Fig. 1, *a*–*d* respectively) were doped with beryllium, while samples 5–8 (Fig. 1, *e*–*h*) were doped with silicon. The growth parameters are summarized in Table. Samples 2, 5 and 8 were grown in two-stage process, when a low-doped core is grown first, then the P flux is increased so that the catalytic cap collapses and vertical growth stops. Then the dopant flux is increased and highly-doped shell is grown. Other samples are grown in a one-step VLS process. Growth temperatures and V/III ratios are chosen so that the dopant incorporation does not preventing the nanowire growth.

Table

Growth parameters

Sample		1	2	3	4	5	6	7	8
Dopant		Be	Be	Be	Be	Si	Si	Si	Si
V/III	step 1	12	12	12	20	30	20	12	30
	step 2	–	30	–	–	12	–	–	39
T_{growth}, °C		640	630	680	640	640	640	610	630

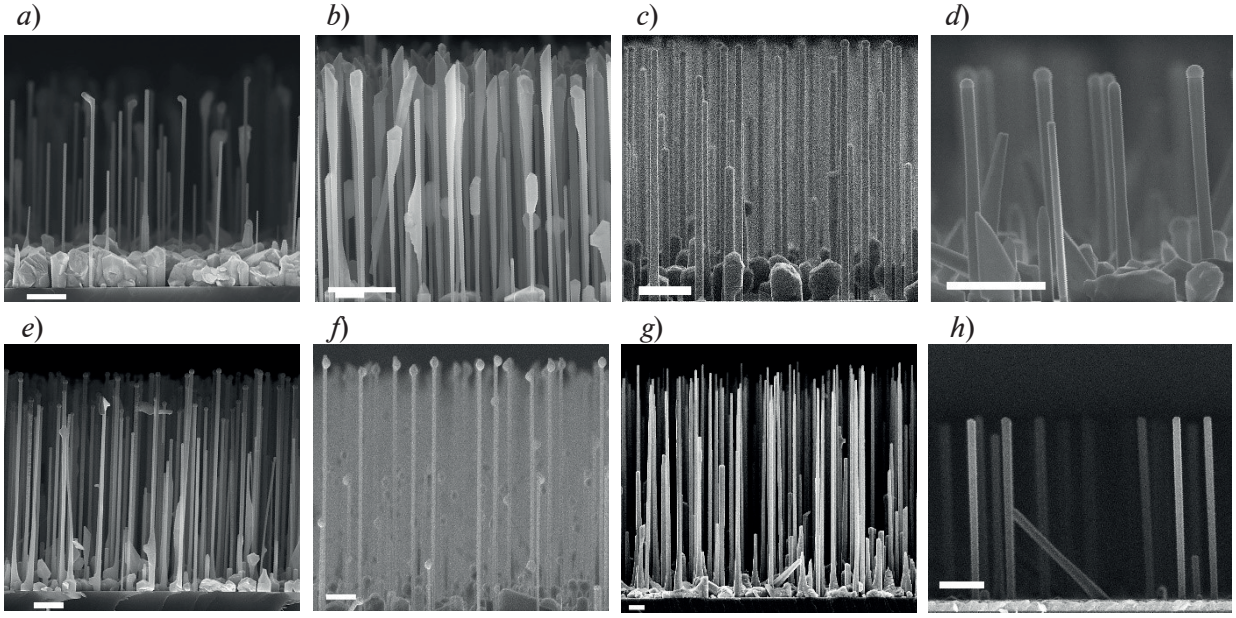

Fig. 1. SEM images of the grown samples. The panels from (*a*) to (*h*) correspond to samples 1–8 from Table
All scale bars are 1 μm long

Individual nanowire *I*–*V* curves of each sample were obtained with C-AFM. The experiment scheme is presented in Fig. 2, *a*. Several nanowires were investigated in each array, average obtained *I*–*V* curves are shown in Fig. 2, *b*. The obtained curves possess low noise level indicating that tip-nanowire electrical contact is stable. The curves were obtained in dark conditions to avoid the impact of photogeneration in Si substrate. All curves show rectifying behavior originating mainly from nanowire/tip Schottky and nanowire/substrate contacts. The curve shape varies significantly from sample to sample. Samples 1, 2, 5 show near-zero current. The most likely explanation for this lies in insufficient diameter of nanowires, so that the surface band bending takes place causing surface depletion which can't be compensated with moderate doping level. Sample 3 also shows near-zero current, indicating that the chosen growth temperature lies beyond the window of Be incorporation, which is in accordance with the literature [9]. Samples 6, 7 show

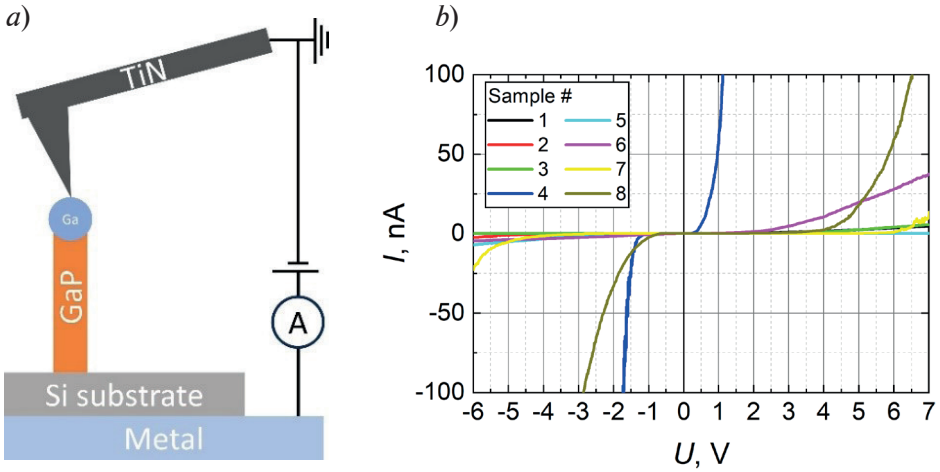

Fig. 2. C-AFM I-V curve measurement scheme (*a*), I–V curves from individual nanowires in each sample (*b*)

moderate current indicating that the doping level is high enough to create a conductive channel in the nanowire core. Samples 4 and 8 demonstrate the highest conductivity, which can be attributed with higher thickness followed by higher dopant incorporation rate.

Then, the numerical modeling of *I–V* curves was carried out in Silvaco TCAD. The nanowire is parametrized with its length *l*, radius *r*, doping level, carrier mobility μ, and GaP band parameters. The tip/nanowire contact is parametrized with Schottky barrier height, depending on probe work function Φ. Length *l* can be well estimated from SEM images while the exact *r* value for the studied wires is unknown, because nanowire thickness dispersion within the same array is pronounced. The accuracy of determining Φ and μ values is also limited. It is known that μ in nanowires can be several orders of magnitude lower than in bulk due to flat defects. Thus, we sweep μ from 0.1 to 20 $cm^2/V{\cdot}s$. We also vary Φ from 4.5 to 5.2 eV based on the estimated values of the probe coatings work function.

Fig. 3 shows modeling results for 2 μm long p-doped nanowire grown on *p*-Si substrate, corresponding to sample 4. The dotted curves correspond to the experimental data. From the figure it follows that shifting carrier mobility, nanowire thickness or work function within physically reasonable range changes the current level within one order of magnitude. The curve shape is mainly governed by the nanowire doping level. 100 nm thick wire is fully depleted if the doping level is less than $1{\cdot}10^{19}$ cm^{-3}. However, increasing N_A twice, from $1{\cdot}10^{19}$ to $2{\cdot}10^{19}$ cm^{-3}, induces the increase of forward current by two orders of magnitude. Comparing the modeling results with the experimental curve from Fig. 2, we estimate the doping level of Sample 4 lies in the range from $1{\cdot}10^{19}$ to $3{\cdot}10^{19}$ cm^{-3}.

Fig. 4 shows the modeled *I–V* curves for 4 μm long *n*-GaP nanowire grown on *n*-Si substrate. The dotted curves correspond to the experimental data. The nanowire is considered to have core/shell structure with low doped core and high doped shell, which corresponds to the case of Sample 8. The core and shell are supposed to have the same thickness varying from 30 to 50 nm. The impact of core doping level N_D^{core} on nanowire conductivity is negligible until it is far less than the doping of the shell. The conductivity is determined by shell doping level N_D^{shell}. Increasing N_D^{shell} from $1{\cdot}10^{18}$ to $1{\cdot}10^{19}$ cm^{-3} leads to the increase of the forward current more than 2 orders of magnitude. Assuming $r_{core} = r_{shell} = 50$ nm, $\mu = 20$ $cm^2/V{\cdot}s$ and $\Phi = 4.9$ eV, the model predicts the doping level of sample 8 on the order of $3{\cdot}10^{18}$, a certain degree of discrepancy of modeled and experimental curves is probably due to more complicated real radial doping distribution and tip/nanowire contact geometry.

The dominating impact of doping level on nanowire conductivity can be explained via the balance between nanowire/substrate heterobarrier and nanowire/probe Schottky barrier. The current depends on the tunneling rate through the barriers, appearing at the high doping levels, rather than on thermionic emission. It should be noted that the proposed model does not take into account the nanowire surface states density and, as a consequence, the appearance of surface band bending on the nanowire side facets causing surface depletion. In fact, the nanowire conductivity

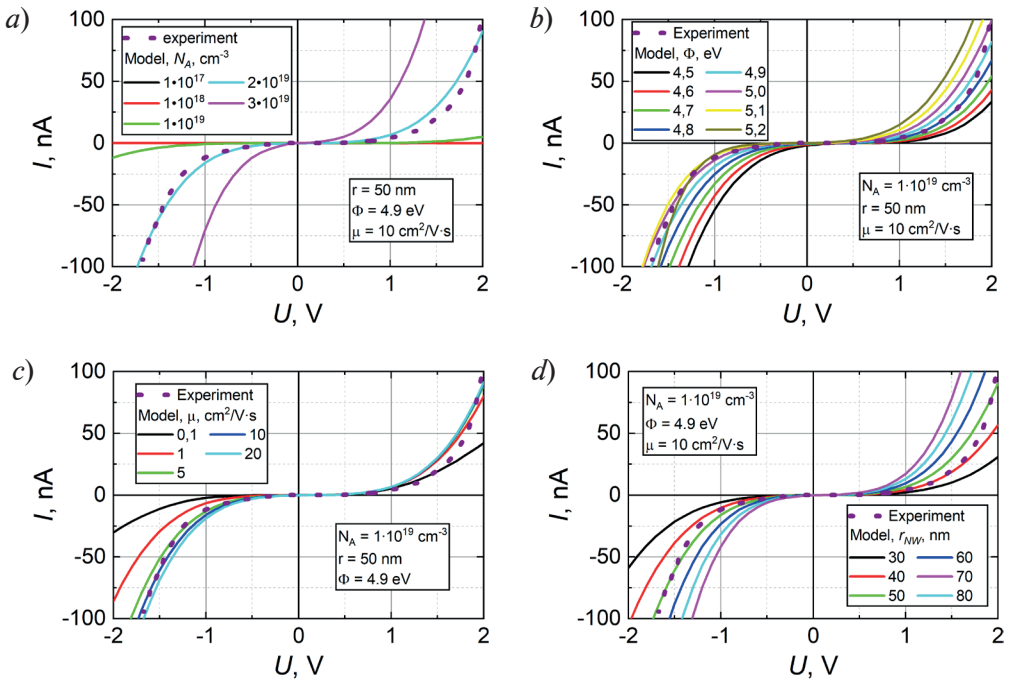

Fig. 3. Numerical modeling of $I-V$ curves from p-GaP nanowire with varying doping level (*a*), work function (*b*), carrier mobility (*c*), radius (*d*)

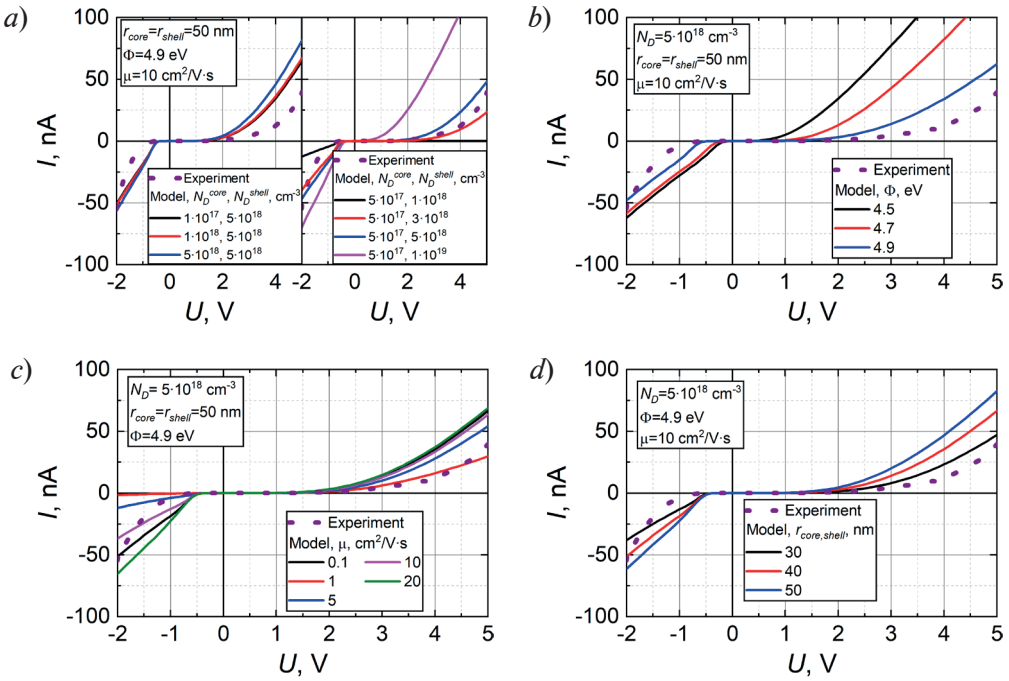

Fig. 4. Numerical modeling of $I-V$ curves from n-GaP nanowire with varying doping level (*a*), Work function (*b*), carrier mobility (*c*), radius (*d*)

is determined by the doping level in conjunction with the nanowire thickness. However, the modeled samples are thick enough and their doping level is high enough so that the radius of surface depletion region is negligible, and the proposed doping estimations are valid.

Conclusion

Conductivity of individual MBE-grown Si- and Be- doped gallium phosphide nanowires is investigated via C-AFM by obtaining $I-V$ curves following by their numerical analysis. The impact of nanowire geometry, doping level, carrier mobility and contact barrier on the conductivity is

studied, the dominating role of the doping level is established. From the experiment it follows that *p*-GaP nanowires with high conductivity can be synthesized under flux ratio V/III = 20 and the growth temperature T_{gr} = 640 °C. The proposed model works well for homogenous Be-doped nanowire giving the doping level on the order of $1 \cdot 10^{19}$ cm^{-3}. In case of two-stage core/shell grown Si-doped nanowires, the model predicts the doping level on the order of $3 \cdot 10^{18}$ cm^{-3}.

Acknowledgments

V.A.S acknowledges support of the electric measurements and numerical modeling by Russian Science foundation (Grant No. 23-72-01082).

REFERENCES

1. **Kuznetsov A., Moiseev E., Abramov A.N., Fominykh N., Sharov V.A., Kondratev V.M., Shishkin I.I., Kotlyar K.P., Kirilenko D.A., Fedorov V.V., Kadinskaya S.A., Vorobyev A.A., Mukhin I.S., Arsenin A.V., Volkov V.S., Kravtsov V., Bolshakov A.D.,** Elastic Gallium Phosphide Nanowire Optical Waveguides—Versatile Subwavelength Platform for Integrated Photonics, Small. 19 (28) (2023) 2301660.

2. **Kim W., L. Güniat L., Fontcuberta A. Morral, Piazza V.,** Doping challenges and pathways to industrial scalability of III–V nanowire arrays, Applied Physics Reviews. 1 (8) (2021) 011304.

3. **Miroshnichenko A.S., Deriabin K.V., Baeva M., Kochetkov F.M., Neplokh V., Fedorov V.V., Mozharov A.M, Koval O.Yu., Krasnikov D.V., Sharov V.A., Filatov N.A., Gets D.S., Nasibulin A.G., Makarov S.V., Mukhin I.S., Kukushkin V.Yu., Islamova R.M.,** Flexible Perovskite $CsPbBr_3$ Light Emitting Devices Integrated with GaP Nanowire Arrays in Highly Transparent and Durable Functionalized Silicones. The Journal of Physical Chemistry Letters, 12 (39) (2021) 9672–9676.

4. **Alekseev P.A., Sharov V.A., Dunaevskiy M.S., Kirilenko D.A., Ilkiv I.V., Reznik R.R., Cirlin G.E., Berkovits V.L.,** Control of Conductivity of $In_xGa_{1-x}As$ Nanowires by Applied Tension and Surface States, Nano Letters. 19 (7) (2019) 4463–4469.

5. **Alekseev P.A., Sharov V.A., Borodin B.R., Dunaevskiy M.S., Reznik R.R., Cirlin G. E.,** Effect of the uniaxial compression on the GaAs nanowire solar cell, Micromachines. 11 (6) (2020) 581.

6. **Sarkar A.,** Device simulation using Silvaco ATLAS tool, in: Technology Computer Aided Design, CRC Press, 2018

7. **Hurkx G.A. M., Klaassen D., Knuvers M.,** A new recombination model for device simulation including tunneling, IEEE Transactions on Electron Devices. 39 (2) (1992) 331–338.

8. **Matsuzawa K., Uchida K., Nishiyama A.,** A unified simulation of Schottky and ohmic contacts, IEEE Transactions on Electron Devices. 47 (1) (2000) 103–108.

9. **Casadei A., Krogstrup P., Heiss M., Röhr J.A., Colombo C., Ruelle T., Upadhyay S., Sørensen C.B., Nygård J., Fontcuberta A. Morral,** Doping incorporation paths in catalyst-free Be-doped GaAs nanowires, Applied Physics Letters. 102 (1) (2013) 013117.

THE AUTHORS

SHAROV Vladislav A.
vl_sharov@mail.ru
ORCID: 0000-0001-9693-5748

FEDOROV Vladimir V.
burunduk.uk@gmail.com
ORCID: 0000-0002-2283-0086

ALEKSEEV Prokhor A.
npoxep@gmail.com
ORCID: 0000-0002-8143-4606

MUKHIN Ivan S.
imukhin@spbau.ru
ORCID: 0000-0001-9792-045X

Received 14.12.2023. Approved after reviewing 12.02.2024. Accepted 18.02.2024.